

## Pyridine-Functionalized Single-Walled Carbon Nanotubes as Gelators for Poly(acrylic acid) Hydrogels

Mustafa K. Bayazit, Lucinda S. Clarke, Karl S. Coleman,\* and Nigel Clarke

Department of Chemistry, Durham University, South Road, Durham DH1 3LE, United Kingdom

Received August 25, 2010; E-mail: k.s.coleman@durham.ac.uk

**Abstract:** Pyridine-functionalized single-walled carbon nanotubes (SWNTs) are prepared from the addition of a pyridine diazonium salt to nanotubes. The location and distribution of the functional groups is determined by atomic force microscopy using electrostatic interactions with gold nanoparticles. The pyridine-functionalized SWNTs are able to act as cross-linkers and hydrogen bond to poly(acrylic acid) to form SWNT hydrogels. The pyridine-functionalized SWNTs are further characterized using Raman, FTIR, UV/vis–NIR, and X-ray photoelectron spectroscopy and thermogravimetric analysis–mass spectrometry.

### Introduction

Carbon nanotubes (CNTs) have a unique place in nanoscience owing to their exceptional electrical, thermal, and mechanical properties and may find application in areas as diverse as composite materials, energy storage, sensors, field emission devices, and nanoscale electronic components.<sup>1,2</sup> For the full potential of CNTs to be realized, much effort has been focused on their surface chemistry. The introduction of surface groups has the obvious advantage of introducing extra functionality to the CNTs, which can be important for sensing and self-assembly in electronic devices or even as points of attachment for polymers or biomolecules. Also the surface groups have the added advantage of interrupting the strong van der Waals forces that cause aggregation or bundling of the material, particularly problematic for single-walled carbon nanotubes (SWNTs), and thus aid dispersion in both aqueous and nonaqueous solvents.<sup>3</sup> Covalent strategies to functionalize CNTs have included carbene,<sup>4</sup> radical,<sup>5,6</sup> cycloaddition,<sup>7–9</sup> and oxidation<sup>10,11</sup> reactions and have been recently reviewed.<sup>12–14</sup> Cycloaddition and radical reactions involving aryl diazonium salts have so far proved to

be the more popular reactions due to their versatility and relative simplicity. The 1,3-dipolar cycloaddition of azomethine ylides has seen widespread use thanks in part to increased solubility in aqueous solutions and the ease in which pharmacologically active molecules such as peptides, plasmid DNA, methotrexate, and amphotericin B can be attached.<sup>8,15–19</sup> The introduction of aryl groups to the surface of CNTs has been achieved using diazonium salts directly<sup>20</sup> or by generation of the aryl diazonium salts in situ by oxidation of the corresponding aniline with inorganic<sup>21</sup> or organic<sup>22</sup> oxidants. The diazonium salt can be activated thermally<sup>22</sup> or electrochemically<sup>23</sup> and the reaction carried out in aqueous<sup>5,20</sup> and nonaqueous<sup>22</sup> solvents or solvent-free conditions.<sup>24</sup>

The use of CNTs in polymer nanocomposites continues to grow. The combination of CNTs with a polymer matrix is expected to improve the thermal, electrical, and mechanical properties of the polymer material. However, dispersion of the CNTs in the host polymer can be difficult, and for this reason efforts have focused on the use of functionalized CNTs in such nanocomposites where the dispersibility of the nanotubes can be improved.<sup>25</sup> CNTs have similarly found use as a reinforcement material for gels, a three-dimensional network of polymer

- (1) Baughman, R. H.; Zakhidov, A. A.; de Heer, W. A. *Science* **2002**, *297*, 787.
- (2) Sun, Y. P.; Fu, K. F.; Lin, Y.; Huang, W. J. *Acc. Chem. Res.* **2002**, *35*, 1096.
- (3) Suri, A.; Chakraborty, A. K.; Coleman, K. S. *Chem. Mater.* **2008**, *20*, 1705.
- (4) Hu, H.; Zhao, B.; Hamon, M. A.; Kamaras, K.; Itkis, M. E.; Haddon, R. C. *J. Am. Chem. Soc.* **2003**, *125*, 14893.
- (5) Price, B. K.; Tour, J. M. *J. Am. Chem. Soc.* **2006**, *128*, 12899.
- (6) Chakraborty, A. K.; Coleman, K. S.; Dhanak, V. R. *Nanotechnology* **2009**, *20*.
- (7) Coleman, K. S.; Bailey, S. R.; Fogden, S.; Green, M. L. H. *J. Am. Chem. Soc.* **2003**, *125*, 8722.
- (8) Tagmatarchis, N.; Prato, M. *J. Mater. Chem.* **2004**, *14*, 437.
- (9) Bayazit, M. K.; Coleman, K. S. *J. Am. Chem. Soc.* **2009**, *131*, 10670.
- (10) Azamian, B. R.; Coleman, K. S.; Davis, J. J.; Hanson, N.; Green, M. L. H. *Chem. Commun.* **2002**, 366.
- (11) Coleman, K. S.; Chakraborty, A. K.; Bailey, S. R.; Sloan, J.; Alexander, M. *Chem. Mater.* **2007**, *19*, 1076.
- (12) Tasis, D.; Tagmatarchis, N.; Bianco, A.; Prato, M. *Chem. Rev.* **2006**, *106*, 1105.
- (13) Peng, X. H.; Wong, S. S. *Adv. Mater.* **2009**, *21*, 625.
- (14) Singh, P.; Campidelli, S.; Giordani, S.; Bonifazi, D.; Bianco, A.; Prato, M. *Chem. Soc. Rev.* **2009**, *38*, 2214.

- (15) Georgakilas, V.; Bourlinos, A.; Gournis, D.; Tsoufis, T.; Trapalis, C.; Mateo-Alonso, A.; Prato, M. *J. Am. Chem. Soc.* **2008**, *130*, 8733.
- (16) Georgakilas, V.; Kordatos, K.; Prato, M.; Guldi, D. M.; Holzinger, M.; Hirsch, A. *J. Am. Chem. Soc.* **2002**, *124*, 760.
- (17) Pantarotto, D.; Briand, J. P.; Prato, M.; Bianco, A. *Chem. Commun.* **2004**, 16.
- (18) Pantarotto, D.; Singh, R.; McCarthy, D.; Erhardt, M.; Briand, J. P.; Prato, M.; Kostarelos, K.; Bianco, A. *Angew. Chem., Int. Ed.* **2004**, *43*, 5242.
- (19) Kostarelos, K.; Lacerda, L.; Pastorin, G.; Wu, W.; Wieckowski, S.; Luangsivilay, J.; Godefroy, S.; Pantarotto, D.; Briand, J. P.; Muller, S.; Prato, M.; Bianco, A. *Nat. Nanotechnol.* **2007**, *2*, 108.
- (20) Strano, M. S.; Dyke, C. A.; Usrey, M. L.; Barone, P. W.; Allen, M. J.; Shan, H. W.; Kittrell, C.; Hauge, R. H.; Tour, J. M.; Smalley, R. E. *Science* **2003**, *301*, 1519.
- (21) Stephenson, J. J.; Hudson, J. L.; Azad, S.; Tour, J. M. *Chem. Mater.* **2006**, *18*, 374.
- (22) Bahr, J. L.; Tour, J. M. *Chem. Mater.* **2001**, *13*, 3823.
- (23) Bahr, J. L.; Yang, J. P.; Kosynkin, D. V.; Bronikowski, M. J.; Smalley, R. E.; Tour, J. M. *J. Am. Chem. Soc.* **2001**, *123*, 6536.
- (24) Dyke, C. A.; Stewart, M. P.; Maya, F.; Tour, J. M. *Synlett* **2004**, 155.
- (25) Coleman, J. N.; Khan, U.; Gun'ko, Y. K. *Adv. Mater.* **2006**, *18*, 689.

chains cross-linked with chemical or physical interactions. Typically the CNTs are added to preformed gels or are present in a reaction mixture where a gelator is added to form the gel. CNTs have been used to support gels of poly(methyl methacrylate),<sup>26</sup> poly(vinyl alcohol),<sup>27</sup> hyaluronic acid cross-linked with divinyl sulfone,<sup>28</sup> and organogels of alanine.<sup>29</sup> There are very few examples where CNTs are directly responsible for gel formation. Poly(ethyleneimine)-functionalized SWNTs have been used to cross-link collagen in the presence of a carbodiimide coupling agent,<sup>30</sup> and cyclodextrin-modified SWNTs have been used to exploit host–guest interactions to form a hydrogel with dodecylated poly(acrylic acid).<sup>31</sup>

Here we report the synthesis of pyridine-functionalized SWNTs via a diazonium-based radical reaction and the ability of the pyridine-functionalized SWNTs to act as a gelator to form hydrogels of poly(acrylic acid). Hydrogels have potential applications as structural biomaterials in areas such as tissue engineering.<sup>28</sup> The pyridine-functionalized SWNT material was characterized by X-ray photoelectron spectroscopy (XPS), thermogravimetric analysis–mass spectrometry (TGA–MS), and UV/vis–NIR, FTIR, and Raman spectroscopy, and the location and distribution of the functional groups were determined using atomic force microscopy (AFM).

## Experimental Details

**Material Preparation. 1. SWNTs.** Purified SWNTs, produced by the HiPco method, were purchased from Unidym and further purified by heating in air at 400 °C and soaking in 6 M HCl overnight. The purified SWNTs were isolated by filtration over a polycarbonate membrane (0.2 μm, Whatman) and washed with copious amounts of high-purity water until pH neutral. The purified SWNTs were annealed under vacuum (10<sup>-2</sup> mbar) at 900 °C to remove residual oxygen-containing functional groups and any adsorbed gases or solvents.

**2. SWNT–Pyridine.** A cooled solution (0 °C) of NaNO<sub>2</sub> (0.490 g, 7.10 mmol) dissolved in 0.7 mL of water was added dropwise to 4-aminopyridine (0.658 g, 6.99 mmol) dissolved in 5 mL of HCl (4 M) cooled to 0 °C. The resulting yellow solution was stirred for 30 min and maintained at 0 °C. A cooled solution (0 °C) of purified SWNTs (10 mg) dispersed in *N,N*-dimethylformamide (20 mL), using an ultrasonic bath (Ultrawave U50, 30–40 kHz) for 5 min, was then added dropwise. The reaction mixture was held at 0 °C and stirred for 4 h, after which time it was allowed to warm to room temperature and stirred for a further 15 h. The SWNTs were filtered through a nylon membrane (0.2 μm, Whatman), redispersed in 2 M HCl (100 mL), filtered, and washed with a copious amount of water until pH neutral. The resulting solid material was dispersed in 2 M NaOH (100 mL) and stirred overnight to ensure deprotonation of the pyridinium salt to pyridine. The functionalized SWNTs were then isolated by filtration through a nylon membrane (0.2 μm, Whatman), washed with water until pH neutral, redispersed and filtered using THF (2 × 30 mL), acetone (2 × 30 mL), and ethanol (2 × 30 mL), respectively, and dried overnight at 80 °C to afford SWNT–pyridine (1).

**Characterization. 1. AFM.** Samples for AFM analysis were produced by drop deposition onto freshly cleaved mica of the

corresponding solution of SWNTs (ca. 0.005 mg mL<sup>-1</sup>) in *N,N*-dimethylformamide produced by sonication in an ultrasonic bath (Ultrawave U50, 30–40 kHz) for 15 min. Samples were dried in air before imaging in tapping mode using a Digital Instruments Multimode AFM instrument with a Nanoscope IV controller.

**2. XPS.** XPS studies were performed at NCESS, Daresbury Laboratory, using a Scienta ESCA 300 hemispherical analyzer with a base pressure under 3 × 10<sup>-9</sup> mbar. The analysis chamber was equipped with a monochromated Al Kα X-ray source ( $h\nu = 1486.6$  eV). Charge compensation was achieved (if required) by supplying low-energy (<3 eV) electrons to the samples. XPS data were referenced with respect to the corresponding C 1s binding energy of 284.5 eV, which is typical for carbon nanotubes.<sup>17</sup> Photoelectrons were collected at a 45° takeoff angle, and the analyzer pass energy was set to 150 eV, giving an overall energy resolution of 0.4 eV.

**3. TGA–MS.** TGA–MS data were recorded on 1–3 mg of sample using a Perkin-Elmer Pyris I coupled to a Hiden HPR20 mass spectrometer. Data were recorded in flowing He (20 mL min<sup>-1</sup>) at a ramp rate of 10 °C min<sup>-1</sup> to 900 °C after being held at 120 °C for 30 min to remove any residual solvent.

**4. UV/Vis–NIR Spectroscopy.** The UV/vis–NIR absorption spectra were recorded on a Perkin-Elmer Lambda 900 spectrometer. The samples were prepared by dispersing the nanotube material in *N,N*-dimethylformamide (ca. 0.03 mg mL<sup>-1</sup>) by sonication in an ultrasonic bath (Ultrawave U50, 30–40 kHz) for 5 min followed by filtration through a plug of cotton wool to remove particulates after the solution was allowed to stand for 2 h.

**5. Raman Spectroscopy.** Raman spectra were recorded using a Jobin Yvon Horiba LabRAM spectrometer in a back-scattered confocal configuration using He/Ne (632.8 nm, 1.96 eV), frequency-doubled Nd:YAG (532 nm, 2.33 eV), or diode (785 nm, 1.58 eV) laser excitation. All spectra were recorded on solid samples over several regions and were referenced to the silicon line at 520 cm<sup>-1</sup>.

**6. Rheology.** Rheology measurements were conducted on a TA Instruments AR2000 using a parallel plate geometry with 40 mm diameter plates and a gap of 1 mm. A frequency sweep from 0.01 to 100 Hz was carried out in controlled strain mode with a strain amplitude of 1%. The concentrations of SWNTs used in the aqueous poly(acrylic acid) dispersions were 1.1 mg mL<sup>-1</sup> for unmodified material and 7.2 mg mL<sup>-1</sup> for pyridine-modified material. These concentrations were chosen as they were the highest concentrations achievable while maintaining a stable dispersion.

**7. SEM.** Hydrogel samples were placed onto precleaned silicon surfaces and briefly submerged in ethanol followed by drying in air. SEM images were taken using an FEI Helios Nanolab 600 operated at 1.5 kV and using secondary electron detection.

## Results and Discussion

**Pyridine-Functionalized SWNTs.** The covalent attachment of aryl groups to the surface of CNTs following the addition and activation of the corresponding diazonium salts is a well-utilized reaction in nanotube chemistry. The mechanism and kinetics of the reaction have been studied, and the reaction has been shown to be selective for metallic SWNTs with the reactivity of the semiconducting SWNTs, which react concurrently but typically more slowly, depending on the diameter of the nanotube and the substituents attached to the aryl ring.<sup>20,32,33</sup> The detailed mechanism of the reaction is complex, and it was only very recently that Chenevier and co-workers showed that it involved a free radical chain reaction with metallic SWNTs having an unexpected catalytic role.<sup>34</sup> Interestingly, although

(26) Vaysse, M.; Khan, M. K.; Sundararajan, P. *Langmuir* **2009**, *25*, 7042.

(27) Tong, X.; Zheng, J. G.; Lu, Y. C.; Zhang, Z. F.; Cheng, H. M. *Mater. Lett.* **2007**, *61*, 1704.

(28) Bhattacharyya, S.; Guillot, S.; Dabboue, H.; Tranchant, J.-F.; Salvétat, J.-P. *Biomacromolecules* **2008**, *9*, 505.

(29) Pal, A.; Chhikara, B. S.; Govindaraj, A.; Bhattacharya, S.; Rao, C. N. R. *J. Mater. Chem.* **2008**, *18*, 2593.

(30) Homenick, C. M.; Sheardown, H.; Adronov, A. *J. Mater. Chem.* **2010**, *20*, 2887.

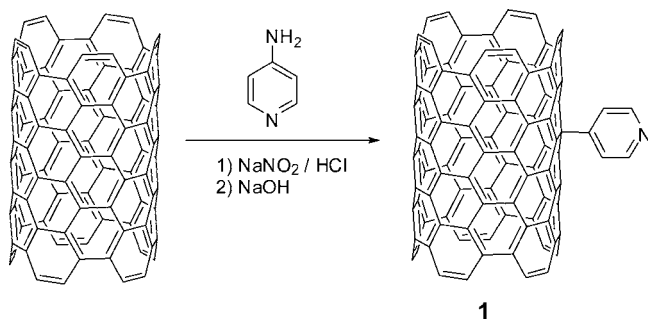
(31) Ogoshi, T.; Takashima, Y.; Yamaguchi, H.; Harada, A. *J. Am. Chem. Soc.* **2007**, *129*, 4878.

(32) Doyle, C. D.; Rocha, J. D. R.; Weisman, R. B.; Tour, J. M. *J. Am. Chem. Soc.* **2008**, *130*, 6795.

(33) Nair, N.; Kim, W. J.; Usrey, M. L.; Strano, M. S. *J. Am. Chem. Soc.* **2007**, *129*, 3946.

(34) Schmidt, G.; Gallon, S.; Esnouf, S.; Bourgoin, J. P.; Chenevier, P. *Chem.–Eur. J.* **2009**, *15*, 2101.

## Scheme 1. Synthesis of Pyridine-Modified SWNTs (1)



the diazonium reaction has been used for the introduction of aryl substituents to CNTs, it has so far not been used to introduce heterocycles to the nanotube surface. This is surprising as the heteroatom introduced could be used to extend CNT chemistry. Here we introduce pyridine groups to the surface of SWNTs and use these groups to form a hydrogel of poly(acrylic acid).

Purified SWNTs were reacted with a pyridine diazonium salt generated in situ by the oxidation of 4-aminopyridine with  $\text{NaNO}_2$  in HCl to afford pyridine-functionalized SWNTs (**1**), Scheme 1. The acidic conditions of the reaction ensure that the pyridine nitrogen is protonated prior to generation of the diazonium salt, preventing oxidation. Therefore, before the free pyridine-modified SWNTs can be isolated, it is necessary to deprotonate the pyridinium salt formed in the initial reaction using sodium hydroxide. UV/vis–NIR spectroscopy of **1** confirmed the covalent attachment of the pyridine functional group to the surface of the nanotube as the characteristic absorption bands corresponding to the electronic transitions between the van Hove singularities were suppressed upon functionalization,<sup>35</sup> Figure 1. From Beer's law, using an extinction coefficient of  $30 \text{ mL mg}^{-1} \text{ cm}^{-1}$  and absorption values at  $\lambda = 700 \text{ nm}$ ,<sup>36</sup> a stable dispersion of **1** in *N,N*-dimethylformamide had a concentration of  $163 \mu\text{g mL}^{-1}$  compared with  $3 \mu\text{g mL}^{-1}$  for unreacted SWNTs. The degree of functionalization of **1** was probed by TGA–MS, which showed a weight loss of 25% at  $600 \text{ }^\circ\text{C}$  compared to ca. 7% for purified SWNTs, Figure 2. This corresponds to the presence of approximately 1 functional group for every 30 nanotube carbon atoms. The peak of mass loss is ca.  $310 \text{ }^\circ\text{C}$  and corresponds to the pyridine fragment (79 amu) which was detected by mass spectrometry. The level of functionalization was confirmed by XPS measure-

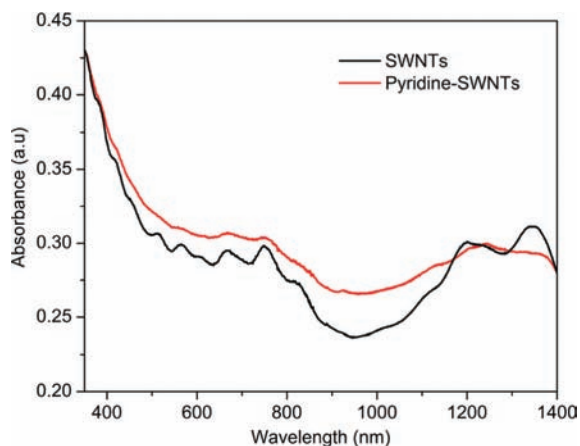


**Figure 1.** Normalized (at 350 nm) UV/vis–NIR spectra, recorded in *N,N*-dimethylformamide, of purified SWNTs (black) and pyridine-functionalized SWNTs (red).

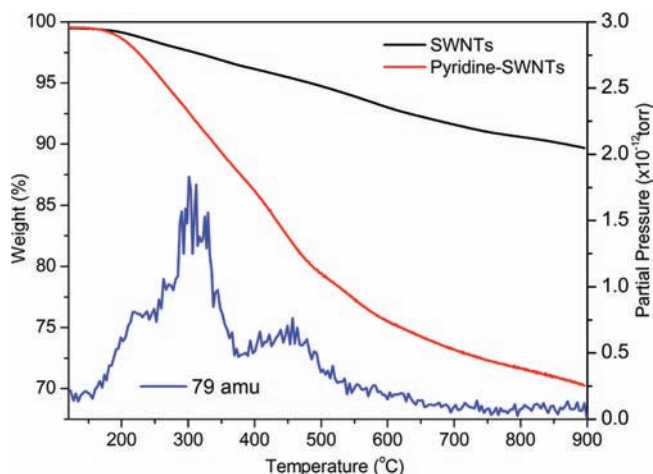


**Figure 2.** TGA–MS data ( $10 \text{ }^\circ\text{C min}^{-1}$ ) of purified SWNTs (black) and pyridine-functionalized SWNTs (red). MS trace (blue) of pyridine (79 amu) given off during heating.

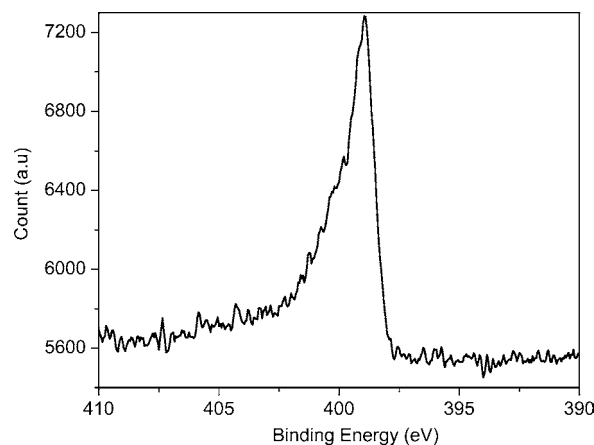


**Figure 3.** N1s X-ray photoelectron spectrum of pyridine-functionalized SWNTs.

ments, where elemental composition analysis showed the presence of ca. 3.0 atom % nitrogen in **1** equivalent to approximately 1 pyridine group per 33 nanotube carbon atoms, which is in close agreement with the TGA–MS data. The N1s binding energy of the pyridine group in **1** is at 398.8 eV and is typical for an  $\text{sp}^2$  nitrogen, Figure 3.

Raman spectroscopy has been used extensively to study SWNTs, with the D-band at ca.  $1350 \text{ cm}^{-1}$  linked to the reduction in symmetry of the SWNTs, the intensity of which offers an approximation of the degree of functionalization when compared with that of the tangential band (G-band) at ca.  $1590 \text{ cm}^{-1}$ .<sup>4,37,38</sup> The Raman spectra (532 nm excitation, 2.33 eV) of **1** and purified SWNTs, for comparison, are shown in Figure 4. The pyridine-modified SWNTs have an enhanced D-band at ca.  $1330 \text{ cm}^{-1}$  when compared with unmodified SWNTs, with an  $A_D/A_G$  ratio of 0.41 versus 0.14 for purified pristine SWNTs, indicative of groups attached to the surface of the nanotubes.

(35) Boul, P. J.; Liu, J.; Mickelson, E. T.; Huffman, C. B.; Ericson, L. M.; Chiang, I. W.; Smith, K. A.; Colbert, D. T.; Hauge, R. H.; Margrave, J. L.; Smalley, R. E. *Chem. Phys. Lett.* **1999**, *310*, 367.

(36) Landi, B. J.; Ruf, H. J.; Worman, J. J.; Raffaele, R. P. *J. Phys. Chem. B* **2004**, *108*, 17089.

(37) Wunderlich, D.; Hauke, F.; Hirsch, A. *J. Mater. Chem.* **2008**, *18*, 1493.

(38) Itkis, M. E.; Perea, D. E.; Jung, R.; Niyogi, S.; Haddon, R. C. *J. Am. Chem. Soc.* **2005**, *127*, 3439.



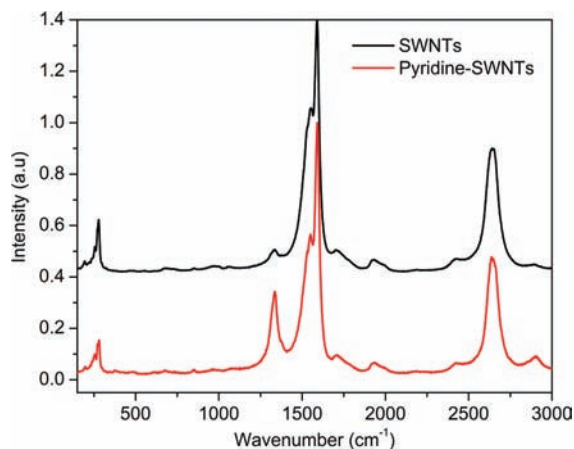


**Figure 4.** Raman spectra (532 nm, 2.33 eV) of purified SWNTs (black) and pyridine-functionalized SWNTs (red) normalized at the G-band ( $1590\text{ cm}^{-1}$ ).

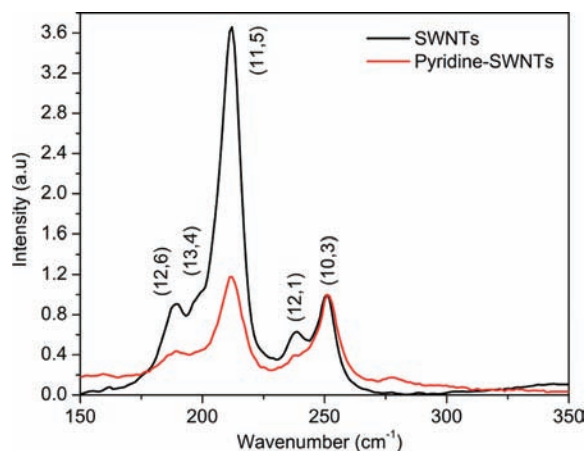


**Figure 5.** RBM region of the Raman spectra (632.8 nm, 1.96 eV) of purified SWNTs (black) and pyridine-functionalized SWNTs (red) normalized at  $251\text{ cm}^{-1}$ .

The rate of reaction of diazonium salts with CNTs has been shown to be fast for metallic SWNTs, with the reactivity of the semiconducting SWNTs exhibiting a more complex relationship with the nanotube diameter and the substituents present on the aryl diazonium salt.<sup>20,32,33</sup> The reactivity of the pyridine diazonium salts appears to be no different. Examination of the radial breathing modes (RBMs) in the Raman spectra at 632.8 nm (1.96 eV) excitation, known to excite both metallic and semiconducting SWNTs, shows some differences between the chemically functionalized and pristine SWNTs, Figure 5. The Raman spectrum of purified SWNTs shows five peaks at ca. 189, 197, 212, 238, and  $251\text{ cm}^{-1}$  in the RBM region which can be assigned to (12,6) (13,4), (11,5), (12,1), and (10,3) SWNTs, respectively, using the modified Kataura plots of Strano,<sup>39</sup> the first three being metallic and the remaining two semiconducting nanotubes. Following normalization at  $251\text{ cm}^{-1}$ , which remained relatively unchanged during the reaction, the band most influenced by the addition of the pyridine diazonium salt was the one at  $189\text{ cm}^{-1}$  (12,6) which corresponds to metallic SWNTs. In contrast, excitation at 785 nm (1.58 eV), which brings into resonance predominately semiconducting SWNTs, showed only minor differences between modified and unmodified SWNTs, Figure 6. Normalization at

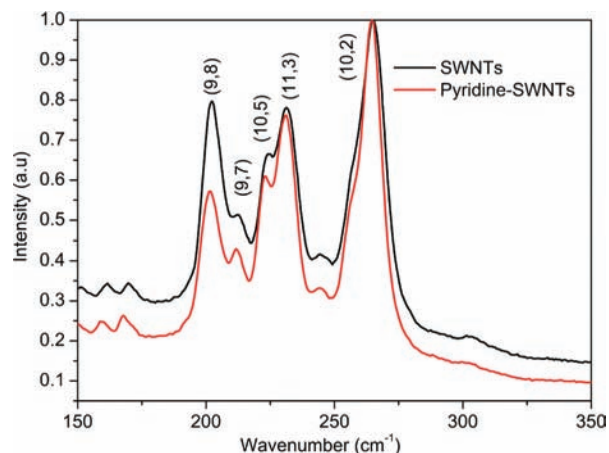
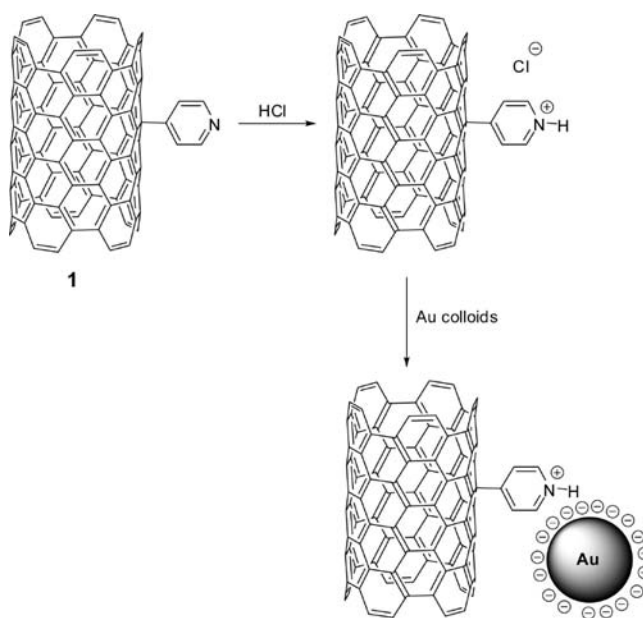


**Figure 6.** RBM region of the Raman spectra (785 nm, 1.58 eV) of purified SWNTs (black) and pyridine-functionalized SWNTs (red) normalized at  $265\text{ cm}^{-1}$ .

**Scheme 2.** Schematic Representation of the Electrostatic Interaction of Gold Colloids with Pyridine-Functionalized SWNTs (1) for AFM Functional Group Tagging Experiments



$265\text{ cm}^{-1}$ , relatively unchanged after the reaction, implies that there may be a small preference for reaction with larger diameter semiconducting SWNTs as the bands assigned to (10,5), (9,7), and (9,8) are slightly reduced in intensity. Excitation at 532 nm (2.33 eV), which is known to bring the metallic SWNTs into resonance, shows the expected decrease in intensity of all bands, when the spectra are normalized to the G-band; see the Supporting Information, Figure S1.

**Functional Group Location.** Information on the location and distribution of functional groups on the nanotube surface can be provided using nanoparticle tagging experiments. We have demonstrated previously that it is possible to exploit the chemistry of the attached organic group to anchor gold nanoparticles to the surface of the SWNTs, allowing the functional groups to be visualized by AFM.<sup>7,9,10</sup> For **1** the methodology is relatively simple and does not require extensive functional group conversion, Scheme 2. Using a strong acid, HCl, it was possible to protonate the pyridine nitrogen to make the corresponding pyridinium salt. Exposing the positively charged pyridinium-

(39) Strano, M. S. *J. Am. Chem. Soc.* **2003**, *125*, 16148.

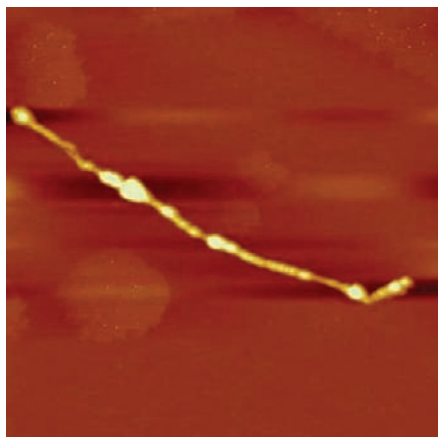


**Figure 7.** A typical tapping mode AFM height image of a protonated pyridine-functionalized SWNT after exposure to citrate-stabilized Au colloids (4–6 nm). The image shown is  $2.0 \mu\text{m}$  by  $2.0 \mu\text{m}$  with a  $z$  scale of 0–5 nm. The Au colloids can be seen (light-colored features) decorating the complete length of the nanotube.

functionalized SWNTs, deposited on a freshly cleaved mica surface, to negatively charged citrate-stabilized gold colloids 4–6 nm in diameter results in an electrostatic interaction of the gold nanoparticles with the functionalized SWNTs, Figure 7. It is clear from the figure that gold particles, visible as light features on the AFM height image, decorate the entire length of the SWNT. Control experiments where purified SWNTs that have not undergone any chemical functionalization are exposed to gold colloids show no significant presence of nanoparticles on the SWNT surface.

**SWNT–Pyridine Hydrogels.** The pyridine-functionalized SWNTs have an accessible heteroatom donor group close to the nanotube surface and are therefore capable of interacting with a variety of materials, in particular functional polymers such as poly(acrylic acid). Poly(acrylic acid) is a pH-responsive polyelectrolyte that has been successfully used to disperse pristine SWNTs in aqueous solutions.<sup>40–43</sup> A stable dispersion in water of  $1.1 \text{ mg mL}^{-1}$  can be achieved. At low pH the SWNTs are said to be completely exfoliated, whereas at high pH (>10) they are only partially exfoliated. Precipitation at high values of pH have also been observed after prolonged periods of time when residual cobalt metal catalyst particles are present.<sup>42</sup> Aqueous solutions of poly(acrylic acid) are protonated at low pH and exhibit a tightly coiled conformation due to intramolecular hydrogen bonding, whereas at high pH poly(acrylic acid) becomes negatively charged due to deprotonation and its conformation becomes extended due to electrostatic repulsion. It is these structural and chemical changes that are responsible for the pH-dependent dispersion behavior of SWNTs with poly(acrylic acid).<sup>41,42</sup>

Dispersing pyridine-functionalized SWNTs in an aqueous solution of 1% poly(acrylic acid) results in a dispersion at the level of  $1.9 \text{ mg mL}^{-1}$  (pH 2.8). This level increases as the pH increases to a maximum of  $7.2 \text{ mg mL}^{-1}$  at pH 5.8; increasing the pH further results in a decrease in the concentration of the

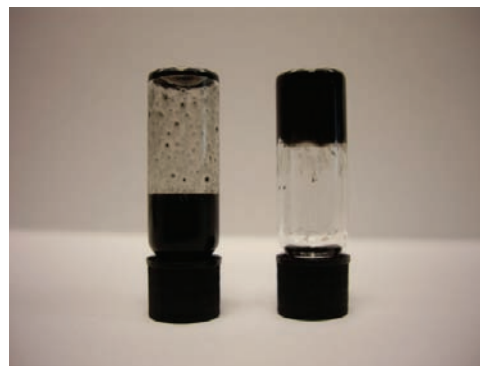


**Figure 8.** Optical photograph of the upturned container test of SWNTs (left) and pyridine-functionalized SWNTs (right) in an aqueous solution of 1% poly(acrylic acid) at pH 5.8.

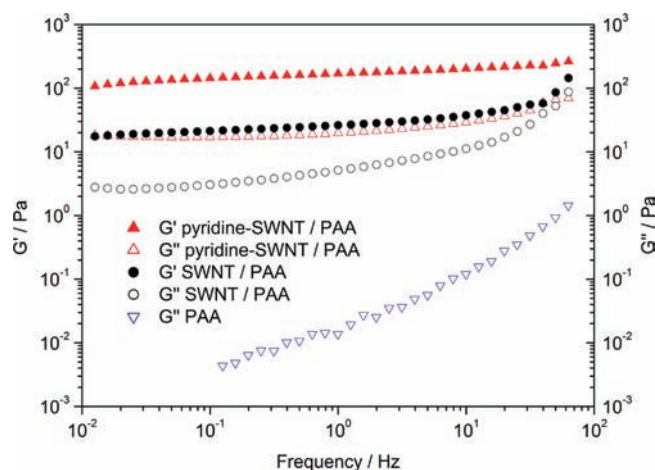


**Figure 9.** Frequency dependence of the storage ( $G'$ , filled symbols) and loss ( $G''$ , unfilled symbols) moduli for 1% poly(acrylic acid) aqueous solution (blue), 1% poly(acrylic acid) aqueous solution containing unmodified SWNTs at pH 5.8 (black), and 1% poly(acrylic acid) aqueous solution containing pyridine-modified SWNTs at pH 5.8 (red). Note that the storage modulus for pure poly(acrylic acid) is not shown since it is below the minimum measurable.

nanotubes until a minimum of  $0.6 \text{ mg mL}^{-1}$  is reached at pH 10.3. The dispersion of pyridine-functionalized SWNTs at pH 5.8 resulted in the formation of a hydrogel that was able to withstand the upturned container test, Figure 8, whereas pristine SWNTs (with concentrations ranging from 1.1 to  $7.2 \text{ mg mL}^{-1}$ ) dispersed in 1% poly(acrylic acid) failed the test and flowed more like a viscous liquid. Rheology measurements confirmed the formation of the hydrogel, Figure 9. Interestingly, it can be seen that the addition of both pristine and pyridine-modified SWNTs significantly increases both the storage and loss moduli as compared to pure aqueous solutions of poly(acrylic acid). In both cases, the storage modulus is reasonably independent of frequency and approximately 1 order of magnitude greater than the loss modulus across the entire frequency range, both of which are signatures of the formation of a rheological gel. However, the storage modulus for the pyridine-modified SWNTs is an order of magnitude greater than that for pristine SWNTs, suggesting a more favorable interaction between the modified nanotubes and the poly(acrylic acid) which can be attributed to hydrogen bonding between the pyridine and carboxylic acid groups holding the network together.

The hydrogel was dried by briefly submerging it in ethanol and allowing the solvent to evaporate. This allowed the gel to

- (40) Grunlan, J. C.; Liu, L.; Kim, Y. S. *Nano Lett.* **2006**, *6*, 911.  
 (41) Grunlan, J. C.; Liu, L.; Regev, O. *J. Colloid Interface Sci.* **2008**, *317*, 346.  
 (42) Tran, N. H.; Milev, A. S.; Wilson, M. A.; Bartlett, J. R.; Kannangara, G. S. K. *Surf. Interface Anal.* **2008**, *40*, 1294.  
 (43) Fagan, J. A.; Landi, B. J.; Mandelbaum, I.; Simpson, J. R.; Bajpai, V.; Bauer, B. J.; Migler, K.; Walker, A. R. H.; Raffaele, R.; Hobbie, E. K. *J. Phys. Chem. B* **2006**, *110*, 23801.

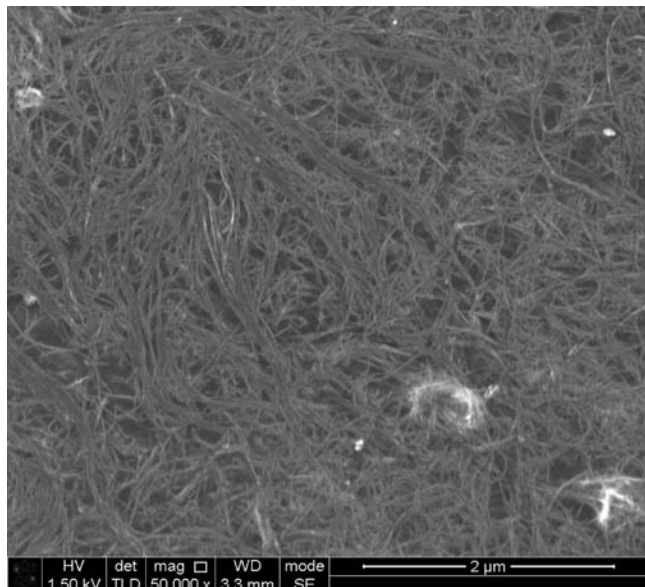


**Figure 10.** SEM image of the dried hydrogel of poly(acrylic acid) containing pyridine-modified SWNTs.

be imaged using SEM, Figure 10. The SEM image shows an extensive network of overlapping nanotubes that are present in bundles ranging from between 50 and 150 nm in diameter. Unfortunately poly(acrylic acid) has a degree of solubility in ethanol, and it is likely that some has been removed during the drying process. However, it is worth noting that the pyridine-modified SWNTs used to form the gel were highly dispersed and predominately individually dispersed as evidence by the fine structure in the UV/vis–NIR spectrum; see the Supporting Information, Figure S2. It is therefore likely that the bundling and cross-linking observed along with the formation of some

fibrous-like material is a consequence of the nanotubes being coated with poly(acrylic acid), which binds the pyridine-modified SWNTs together.

### Conclusion

We have shown that it is possible to introduce pyridine functional groups to the surface of SWNTs via reaction with a pyridine diazonium salt generated in situ. By deliberately protonating the pyridine nitrogen and exploiting the electrostatic interaction with negatively charged citrate-stabilized gold nanoparticles, we have been able to show by AFM the location and distribution of the functional groups on the nanotube surface. The pyridine-functionalized SWNTs acted as gelators for the pH-responsive polyelectrolyte poly(acrylic acid). Hydrogen bonding between the pyridine groups on the SWNTs and the carboxylic acid groups on the polymer were responsible for holding the network together and stabilizing the formation of an SWNT–poly(acrylic acid) hydrogel.

**Acknowledgment.** We thank Dr. Graham Beamson of the National Centre for Electron Spectroscopy and Surface Analysis (NCESS) at Daresbury Laboratory for technical assistance and useful discussions on the XPS measurements, Leon Bowen of the Durham Centre for Electron Microscopy for assistance with SEM, Doug Carswell for recording the TGA data, and the EPSRC (Grant EP/E025722/1) and TUBITAK (M.K.B.) for funding.

**Supporting Information Available:** Figures showing the RBM region of the Raman spectra of purified and pyridine-functionalized SWNTs and UV/vis–NIR spectra of pyridine-functionalized SWNTs in a poly(acrylic acid) aqueous solution and an additional note regarding the TGA of pyridine-functionalized SWNTs. This material is available free of charge via the Internet at <http://pubs.acs.org>.

JA1076662